

# OPTIMUM NOZZLE CONTOURS FOR AEROSPIKE NOZZLES USING A FORTRAN 77

Pires, M., manoloneuzalucas@yahoo.com.br

Universidade Federal do Rio Grande do Sul-Porto Alegre-RS

**Abstract.** A Computer Program in ForTran-77 is developed as primary tool in applying the liquid rocket thrust chamber performance prediction methodology. The code allows improvements incorporated of the Nozzle Contour Optimization to be used as a powerful design tool, as well as an analysis program. The conventional approach to design a nozzle configuration incorporates a RAO technique, which generates an optimum nozzle contour for an inviscid flow for a perfect gas with a constant isentropic exponent. An alternative method uses an optimum truncated 'perfect' nozzle solution. Both of these methods ignore the effects of kinetics, boundary layer losses, base pressure, and external flow interaction. The recent interest in the linear aerospike engine emphasizes the need to include the preceding effects when optimizing for system performance, since the interaction of the free stream with the inviscid flow and boundary layer tend to dominate the overall performance.

**Keywords:** Aerospike, Plug Nozzle, Thrust Coefficient

## 1. INTRODUCTION

Figure 1, summarizes the principle flow phenomena of plug nozzles with full length and truncated central bodies at off-design (top and bottom) and design (center) pressure ratios observed in experiments and numerical simulations (Hagemann et al., 1998). For pressure ratios lower than the design pressure ratio of a plug nozzle with a well-contoured central body, the flow expands near the central plug body without separation, and a system of recompression shocks and expansion waves adapts the exhaust flow to the ambient pressure  $p_{amb}$ .

The characteristic barrel-like form with several inflections of the shear-layer results from various interactions of compression and expansion waves with the shear layer, and turbulent diffusion enlarges the shear layer farther downstream of the throat. The existence of the overexpansion and recompression processes is inferred from up - and down-variations of plug wall pressure profiles observed in various cold-flow tests and numerical simulations. At the design pressure ratio (see Fig. 1, left column, center), the characteristic with the design Mach number should be a straight line emanating to the tip of the central plug body, and the shear layer is parallel to the centerline.

## 2. STEADY TWO-DIMENSIONAL TRANSONIC FLOW IN AEROSPIKE NOZZLES

The determination of the flow pattern in the throat region of a 2-d aerospike nozzle under choked conditions may be accomplished by applying small perturbation techniques to the equations governing the choked flow Zucrow (1977) and Wisse (2005). Of the several methods that have been proposed for analyzing the flow field in the throat region of a two-dimensional nozzle, that due to Sauer (1947) is the simplest. Figures 2 and 3 illustrate schematically the general features of the throat region of a aerospike nozzle. The contour of the nozzle is symmetrical with respect to the axis  $x$ , and it is assumed that the fluid flows in positive direction of the  $x$  axis. Figure 3 it is anticipated that the cross-section of the sonic surface, termed the *sonic line*, is a parabola; It is seen in Figure 3 that the sonic line starts from the wall of the nozzle at a point slightly upstream from the *throat* G, the minimum flow area, proceeds downstream, and crosses the centerline of the nozzle at point 0. Point 0 denotes the origin of the coordinate system employed in the analysis due to Sauer(1942). It corresponds to the intersection of the sonic line with the  $x$  axis. The location of point 0, the distance  $\epsilon$  downstream from the throat G, is determined from the analysis. For either a two-dimensional planar or axisymmetric irrotational flow, the perturbation equation is Zucrow (1977):

$$(1 - M_{\infty}^2)u_x + v_y + \delta \frac{v}{y} = M_{\infty}^2(\gamma + 1)\left(\frac{u}{U_{\infty}}\right)u_x \quad (1)$$

where,  $\delta=0$  for a planar flow and  $\delta=1$  for an axisymmetric flow. Because the flow in the throat region is 1-d and sonic, the undisturbed free-stream velocity  $U_{\infty} = a^*=1 \Rightarrow$  Mach number  $M_{\infty}=1$ . Substituting into equation (1), obtain:

$$(\gamma + 1)\left(\frac{u}{a^*}\right)u_x - v_y - \delta \frac{v}{y} = 0 \quad (2)$$

By definition, let  $u' = u / a^*$  and  $v' = v / a^*$ , Where  $u'$  and  $v'$  are termed the *nondimensional perturbation velocity components*. Introducing  $u'$  and  $v'$  into Equation (2) transforms it to:

$$(\gamma + 1)u'u'_x - v'_y - \frac{v'}{y} = 0 \quad (3)$$

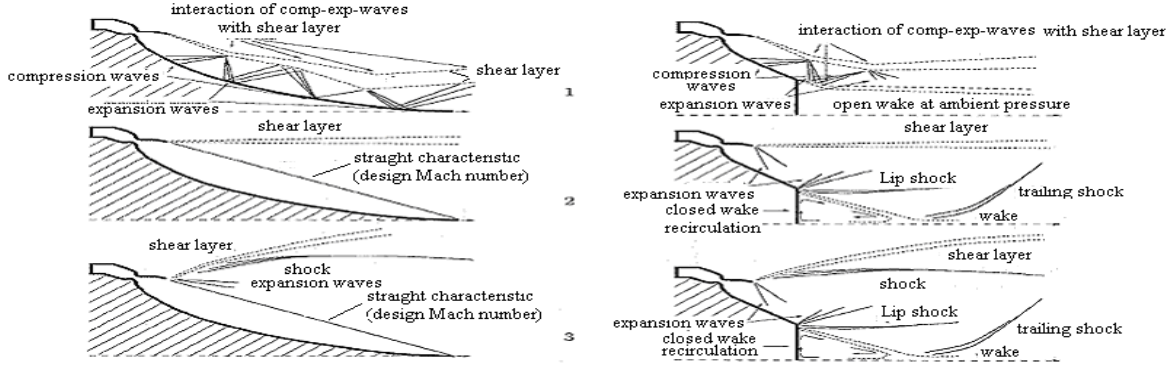


Figure 1 Flow Phenomena of a Aerospike Nozzle and Truncated Body [Plug] at Different Pressure ratio  $p_0/p_{atm}$ . Off-Design (top,bottom) and Design center) Pressure Ratio from Hagemann et al.(1998)



Figure 2 Aerospike Nozzle

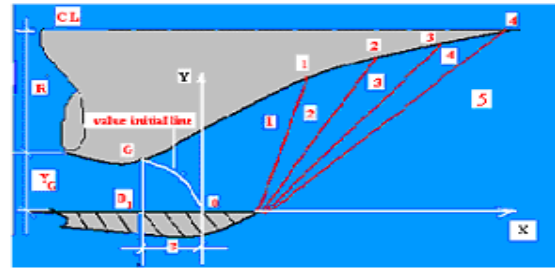


Figure 3 Geometric of the Throat and Coordinate System

Since the flow in the throat region is irrotational, it is possible to define a potential function  $\phi$  for the velocity. Hence, by definition :

$$\Phi = U_{\infty} x + \phi = a^* (x + \phi') \quad (4)$$

where  $\phi'$  is the *nondimensional perturbation velocity potential*. Consequently,

$$\tilde{u} = a^* + u = a^* (1 + u') = \Phi_x = a^* (1 + \phi') \quad (5)$$

$$\tilde{v} = v = a^* v' = \Phi_y = a^* \phi'_y \quad (6)$$

where  $u = \phi'_x$  and  $v = \phi'_y$ . Substituting Equations (5) and Equation (6) into Equation (3), obtain:

$$(\gamma + 1)\phi'_x \phi'_{xx} - \phi'_{yy} - \delta \frac{\phi'_y}{y} = 0 \quad (7)$$

Equation (7) is the governing equation for the *nondimensional perturbation velocity potential for a transonic flow*. His solution is given by Zucrow and Holmann (1977) . Thus,

$$\phi(x, y) = \sum_{i=0}^n f_{2i}(x) y^{2i} = f_0(x) y^0 + f_2(x) y^2 + f_4(x) y^4 + \dots \quad (8)$$

where  $y^0 = 1$ . The corresponding expressions for terms  $\phi'_x, \phi'_{xx}, \phi'_y$  and  $\phi'_{yy}$  are accordingly

$$\phi'_x = f'_0(x) + f'_2(x)y^2 + f'_4(x)y^4 + \dots \quad (9)$$

$$\phi'_{xx} = f''_0(x) + f''_2(x)y^2 + f''_4(x)y^4 + \dots \quad (10)$$

$$\phi'_y = 2f_2(x)y + 4f_4(x)y^3 + \dots \quad (11)$$

$$\phi''_y = 2f_2(x) + 12f_4(x)y^2 + \dots \quad (12)$$

where  $f'_0(x)$  denotes  $df_0(x)/dx$ , and so forth. Substituting the above expressions into Equation (7) and rearranging the result, yields the following polynomial in  $y$ . Thus,

$$y^0[(\gamma+1)f'_0f''_0 - 2f_2 - 2\delta f_2] + y^2[(\gamma+1)(f'_0f''_2 + f''_0f'_2) - 12f_4 - 4\delta f_4] + y^4[\dots] = 0 \quad (13)$$

Since the polynomial Equation (13) must be satisfied for all arbitrary values of  $x$  and  $y$ , the coefficients of each power of  $y$  must be identically zero. Sauer, (1947) truncated the series after the  $f_4(x)y^4$  term. Setting the coefficients of  $y^0$  and  $y^2$  equal to zero and solving for  $f_2(x)$  and  $f_4(x)$  yields:

$$f_2(x) = \frac{(\gamma+1)f'_0f''_0}{2(1+\delta)} \quad (14)$$

$$f_4(x) = \frac{(\gamma+1)(f'_0f''_2 + f''_0f'_2) - 12f_4 - 4\delta f_4}{4(3+\delta)} \quad (15)$$

This  $f_2(x)$  and  $f_4(x)$  may be determined from the derivatives of  $f_0(x)$ . When  $y=0$ ,  $u'(x,0) = f'_0(x)$ , where  $u'(x,0)$  defines the nondimensional perturbation velocity distribution along the  $x$  axis. Consequently, knowing  $u'(x,0)$ , one can determine  $f_2(x)$  and  $f_4(x)$  from Equations (14) and (15), and, therefore, the flow field. If the axial perturbation velocity distribution is assumed to be linear,  $u'(x,0)$  is given by:

$$u'(x,0) = f'_0(x) = \alpha x \quad (16)$$

where  $\alpha$  is a constant, termed the coefficient of the linear nondimensional axial perturbation velocity. Substituting Equation (16) into Equations (14) and (15) gives:

$$f_2(x) = \frac{(\gamma+1)\alpha^2 x}{2(1+\delta)} \quad (17)$$

$$f_4(x) = \frac{(\gamma+1)\alpha^3}{8(1+\delta)(3+\delta)} \quad (18)$$

Substituting equations (17) and (18) into equation (8), yields

$$\phi'(x,y) = f_0(x) + \frac{(\gamma+1)\alpha^2 xy^2}{2(1+\delta)} + \frac{(\gamma+1)\alpha^3 y^4}{8(1+\delta)(3+\delta)} \quad (19)$$

Substituting equation (19) into equations (5) and (6) yields:

$$u'(x,y) = \alpha x + \frac{(\gamma+1)\alpha^2 y^2}{2(1+\delta)} \quad (20)$$

$$v'(x,y) = \frac{(\gamma+1)\alpha^2 xy^2}{2(1+\delta)} + \frac{(\gamma+1)\alpha^3 y^3}{2(1+\delta)(3+\delta)} \quad (21)$$

Equations (20) and (21) yield the *nondimensional perturbation velocities* for a linear axial perturbation velocity distribution. The critical curve where  $M=1$  and  $(\tilde{u}^2 + \tilde{v}^2) = a^{*2}$  may be determined as follows. First, substitute the definition of nondimensional perturbation velocities. Thus,

$$(\tilde{u}^2 + \tilde{v}^2) = a^{*2} = (a^* + u)^2 + v^2 = a^{*2} [(1 + u')^2 + v'^2] \quad (22)$$

Dividing through by  $a^{*2}$  yields:

$$(1 + u')^2 + v'^2 = 1 \quad (23)$$

Expanding Equation (23) and neglecting powers of  $u'$  and  $v'$  yields:  $u' = 0$ , consequently, the Critical curve where  $M=1$  is established by setting  $u' = 0$  in equation (20). Thus,

$$x = -\frac{(y + l)\alpha y^2}{2(l + \delta)} \quad (24)$$

Next, it is necessary to locate the origin of the coordinate system in the nozzle. From Figure 3 it is seen that  $\tilde{v} = v = v' = 0$  in  $x = \varepsilon$  and  $y = y_t$ . Substituting those values for  $x$  and  $y$  into equation (21) yields:

$$\varepsilon = -\frac{(y + l)\alpha y_t^2}{2(3 + \delta)} \quad (25)$$

Equation (25) locates the origin of the coordinate system relative to the nozzle throat.

### 3. DETERMINATION OF THE NOZZLE CONTOUR

Figure 4 illustrates the geometric model employed for determining the curvature  $k$  of the nozzle wall at the narrowest cross-section (throat). From Figure 4:

$$\tan \tau = \frac{v'}{(1 + u')} \equiv v' \quad (26)$$

At the point T, the curvature  $k$  is given by

$$k = \frac{1}{\rho_t} = \left( \frac{d(\tan \tau)}{ds} \right)_T = \left( \frac{dv'}{ds} \right)_T \quad (27)$$

To the differentiate  $dv'/ds$  one may write

$$\frac{dv'}{ds} = v'_x \left( \frac{dx}{ds} \right) + v'_y \left( \frac{dy}{ds} \right) \quad (28)$$

Considerer a nozzle throat with a radius of curvature  $\rho_t$ , which is large compared to the throat radius  $y_t$ .

Hence,  $\rho_t \gg y_t$ ,  $(dx/ds) \cong 1$ , and  $(dy/ds) \cong 0$ . Accordingly, Equation (28) :

$$\frac{dv'}{ds} = v'_x \quad (29)$$

$$\rho_t = \frac{1}{|v'_x(x, y)|_T} = \frac{1}{v'(\varepsilon, y_t)} \quad (30)$$

From equation (21)  $v'_x$  is given by

$$v'_x = \frac{(\gamma+1)\alpha^2 xy^2}{2(1+\delta)} \quad (31)$$

The value of  $v'_x$  at the point T, where  $x = \varepsilon$  and  $y = y_t$ , may be determined from equation (31), one obtains the following Equation (31). Substituting that result into Equation (30), one obtains the following equation for the radius of curvature  $\rho_t$ . Thus,

$$\rho_t = \frac{(1+\delta)}{(\gamma+1)\alpha^2 y_t} \quad (32)$$

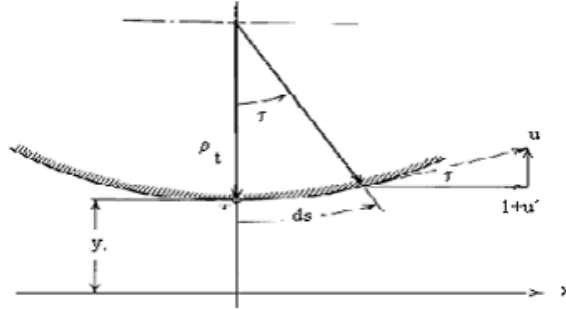


Figure 4 Model for relating the Throat Radius of Curvature to the Flow Field

Solving equation (32) for  $\alpha$  yields:

$$\alpha = \left| \frac{(1+\delta)}{(\gamma+1)\rho_t y_t} \right|^{1/2} \quad (33)$$

Substituting equation (33) for  $\alpha$  into equation (25) yields the following equation for  $\varepsilon$ . Thus,

$$\varepsilon = -\frac{y_t}{2(3+\delta)} \left| \frac{(\gamma+1)(1+\delta)}{(\rho_t / y_t)} \right|^{1/2} \quad (34)$$

#### 4. INITIAL-VALUE LINE FOR SUPERSONIC FLOW FIELD CALCULATIONS

To initiate for the two-dimensional supersonic flow field by the method of characteristics, a line along which  $M > 1$  across the entire throat is needed. The sonic line determined by Sauer's Method (1947) is unsuitable because Mach lines from the sonic line intersect the nozzle wall upstream from the throat point T. Because point T was employed as a boundary condition in the evaluation Equation (32), the region of the flow field upstream from point T is within the range of influence of point T, and the method of characteristics cannot be initiated from an *initial-value line* that is in range of influence of downstream point. The line where  $\tilde{v} = 0$ , which is only a slight distance further downstream than the sonic line, may be employed as an *initial-value line* for the method of characteristics. The equation of the line, which is the locus for  $\tilde{v} = 0$ , is obtained from equation (21) by setting  $v' = 0$ . Thus,

$$x = -\frac{(\gamma+1)\alpha y^2}{2(3+\delta)} \quad (35)$$

#### 5. MASS FLOW RATE AND THRUST

Mass flow rate cross the  $v=0$  line, is given by Zucrow and Holmann (1977). The actual integration of equation (36) is accomplished by applying Simpson's rule. Dividing the integration interval NPI-1 equal subintervals, yields the following algorithm:

$$\dot{m} = 2\pi \left( \frac{\Delta y}{3} \right) \sum_{i=1}^{NPI} C_i (\rho \tilde{u} y)_i \quad \text{where } C_i = 1, 4, 2, \dots, 2, 4, 1 \text{ and } \Delta y = \frac{\rho_t}{NPI-1} \quad (36)$$

Thrust across the  $v=0$  line.

O thrust is the sum of the pressure forces and the momentum flux, Zucrow and Holmann (1977). Equation (37) may be integrated by Simpson's rule. Thus,

$$F = 2\pi \left( \frac{\Delta y}{3} \right) \sum_{i=1}^{NPI} C_i \left[ (p + \rho \tilde{u}^2) y \right]_i \quad (37)$$

Mass flow rate  $\dot{m}$  crossing the element of area  $dA$  (Aerospike nozzle) is given by Pires(1996):

$$\dot{m} = 2\pi \int_0^{y_i} \left( R + \rho_t - \frac{dy}{2} - y \right) dy \quad (38)$$

$$\text{where } r = R + \rho_t - \frac{dy}{2} - y \quad (39)$$

Substituting equation (39) into Equation (38) and neglecting  $dy^2$  obtain:

$$\dot{m} = 2\pi \int_0^{y_i} \left( R + \rho_t - \frac{dy}{2} - y \right) dy \quad (40)$$

The actual integration of Equation (40) is accomplished by applying Simpson's rule. Dividing the integration interval  $NPI-1$  subintervals yields the following algorithm.

$$\dot{m} = 2\pi \left( \frac{\Delta y}{3} \right) \sum_{i=1}^{NPI} C_i [\rho u (R + y)]_i \quad (41)$$

Similarly for thrust in aerospike nozzle

$$F = 2\pi \left( \frac{\Delta y}{3} \right) \sum_{i=1}^{NPI} C_i \left[ (p + \rho u^2) (R + y) \right]_i \quad (42)$$

To determined flow field or the plug nozzle is admitted isentropic expansion of the jet to the final pressure produces a jet Mach number  $M$ , and if  $\gamma$  is the ratio of specific heats, then the angle of refraction is:

$$v = \sqrt{\frac{\gamma+1}{\gamma-1}} \tan^{-1} \sqrt{\frac{\gamma-1}{\gamma+1} (M^2 - 1)} - \tan^{-1} \sqrt{M^2 - 1} \quad (43)$$

Based upon a value of  $v = \text{Mach } 1$ . In Aerospike Nozzle of the type shown in Figure 2 all the supersonic expansion occurs externally. It is of course possible, and in many cases advantageous, to piece to the total expansion between internal and external expansion Berman,(1960). If assume that the internal expansion is a simple corner expansion, the total expansion angle is the sum of the internal and external expansions:

$$v = (\theta_2 - \theta_1) \pm (\theta_2 - \theta_3) \quad (44)$$

where  $v$  is called the Prandtl-Meyer angle.

## 6. SOLUTION METHOD

The basic contour design of the linear aerospike nozzle is in principle based on the application of the inviscid irrotational supersonic Prandtl-Meyer flow theory (1908) derived from the Euler equations. The contour is two-dimensional, since the segments are placed linearly next to each other. The determination of the contour surface of the aerospike nozzle is done of the form where the direction of a frictionless wall is changed by an angle  $\delta$  at the point where the incident expansion wave impinges on it. No reflected wave is required for causing the streamlines crossing wave to become parallel to the surface. The incident expansion wave ends at the surface because its inclination is such

that the reflected wave is neutralized or canceled. i.e., if a weak wave of the angle  $\Delta\theta$  incident about the surface of aerospike nozzle, a reflection wave equal strength must be present of the form to satisfy the boundary condition in surface of the aerospike nozzle. Similarity obtain all points on the aerospike nozzle. If we know the position and the properties of a point on the wall, we can easily determine those of the adjacent point until we reach the exit section point. The plug nozzle Figure 3 is designed admitting design pressure in 5 region equal ambient pressure in a determined altitude of the flight. In this case, how the waves splitting the regions are equal families, hence, the waves of the fan expansion of Prandtl-Meyer are equal strength.

$$\Delta\theta = -\Delta v \quad (45)$$

Of the 1 region to 2 region there is one Mach line or characteristic of same family. Thus

$$\begin{aligned} \theta_2 - \theta_1 &= -v_2 - v_1 = -\Delta v \\ \theta_2 &= \theta_1 - \Delta v \\ \theta_3 &= \theta_1 - 2\Delta v \\ &\dots\dots\dots \\ \theta_n &= \theta_1 - (n-1)\Delta v \end{aligned} \quad (46)$$

$$\text{Where } \Delta v = \frac{v_5 - v_1}{5}$$

$$\begin{aligned} \alpha_{1,1} &= \arcsen \frac{1}{M_1} + \theta_1 & \alpha_{1,2} &= \theta_1 \\ \alpha_{2,2} &= \arcsen \frac{1}{M_2} + \theta_2 & \text{with } \alpha_{2,2} &= \theta_2 \\ &\dots\dots\dots & & \\ \alpha_{n,1} &= \arcsen \frac{1}{M_n} + \theta_n & \alpha_{n,2} &= \theta_n \end{aligned} \quad (47)$$

$$\text{where } \alpha_{i,j} \text{ i = region, j = angle } \alpha \text{ with } i,j = 1 \dots n \quad dx = \frac{dix \cdot \tan \alpha_{2,1} - dify}{\tan \alpha_{2,2} - \tan \alpha_{2,1}} \quad (48)$$

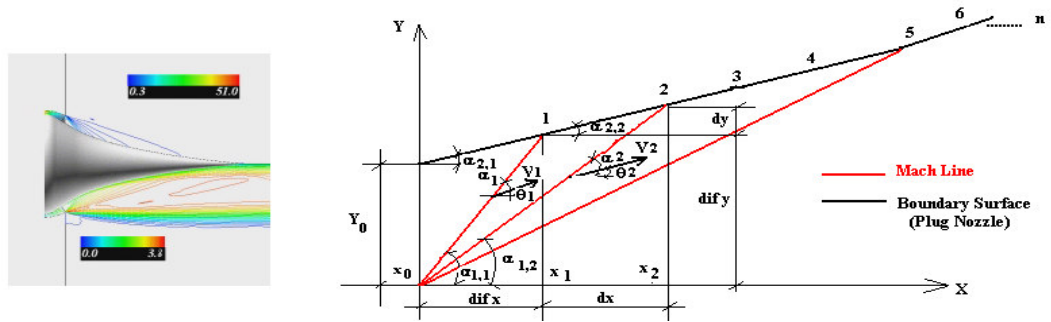


Figure 5 a): Contour plots of pressure (upper half) and Mach number (lower half) distributions ( Pressure Ratio 71) Ito at al (1999) b) Mach Lines

Thus, knowing all coordinate and angle of the points on wall with the axis line, determine the ordinate  $Y_{cc}$  of the radius cone of the aerospike nozzle. Figure 6b

$$y_{cc} = (x_1 - x_0) \tan \theta_1 + (x_2 - x_1) \tan \theta_2 + \dots\dots\dots \quad (49)$$

Equation (49) is applicable for all n Mach lines. Variation of the Thrust on Aerospike nozzle, Pires, (1996) is given by:

$$DF = \pi [(P_w - P_{amb}) (R - y_w) + (P_i - P_{amb}) (R - y_i)] y_i - y_w \quad (50)$$

## 7.RESULT

Pires(1996), Lee (1963 and 1964) developed computational codes written in Fortran 77 to analyse different nozzle concepts with improvements in performance as compared to conventional nozzle achieved by altitude adaptation and, thus, minimizing losses caused by over-or underexpansion. The aerospike nozzle provides, at least theoretically a continuous altitude adaptation up to their geometrical area ratio. The Figure 6 shows the thrust coefficient ( $C_F$ ) of the aerospike Nozzle plotted against the pressure ratio. The solid red line denote the ideal thrust coefficient and the dashed green line the theoretical  $C_F$  of the conventional nozzle. In the low pressure ratio region, the standard nozzle not produce as much thrust as the aerospike nozzle (blue line). That is the reason for higher performance of the aerospike nozzle at lower altitudes.

## 8. CONCLUSION

The results clearly showed the main advantages of the aerospike nozzle. Conventional Bell-type rocket nozzles, which are in use in practically all of today's rockets, limit the overall engine performance during the ascent of the launcher owing to their fixed geometry. Significant performance losses are induced during the off-design operation of the nozzles, when the flow is overexpanded during low-altitude operation with ambient pressures higher than the nozzle exit pressure, or underexpanded during high-altitude operation with ambient pressures lower than the nozzle exit pressure. In the case of overexpanded flow, oblique shocks emanating into the flow field adapt the exhaust flow to the ambient pressure. Further downstream, a system of shocks and expansion waves leads to the characteristic barrel-like form of the exhaust flow. In contrast, the underexpansion of the flow results in a further expansion of the exhaust gases behind the rocket. Off-design operations with either overexpanded or underexpanded It is shown that significant performance gains result from the adaptation of the exhaust flow to the ambient pressure

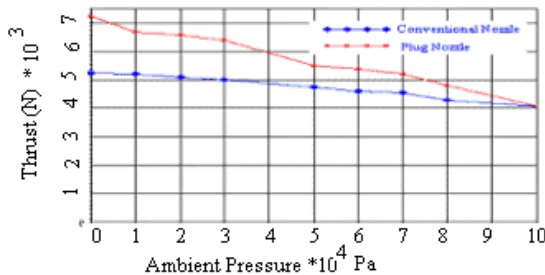


Figure 7 Ambient Pressure (Pa) versus Thrust (N)

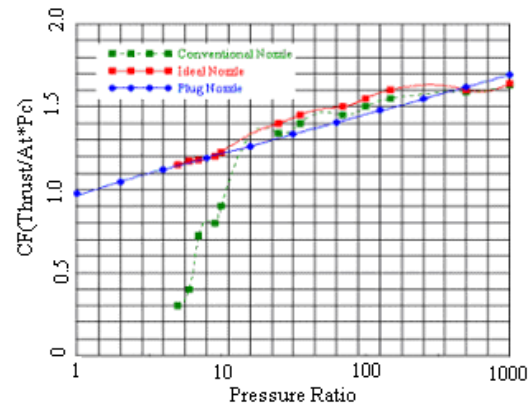


Figure 8 Pressure Ratio Versus Thrust Coefficient

## 9. REFERENCES

- Back L.H., et al, September, 1965 "Comparison of Measured and Predicted Flows through Conical Supersonic Nozzles, with Emphasis on the Transonic Region", Journal of American Institute of Aeronautics and Astronautics, Vol.3, No.9, pp 1606-1614.
- Berman, K. and Crimp, J.F.W., 1960 "Performance of Plug-Type Rocket Exhaust Nozzles" ARS Solid Propellant Rocket Research Conference, Princeton, N.J.
- Ito T. et al. "Computations of the Axisymmetric Plug Nozzle Flow Fields- Flow Structures and Thrust Performance - 17th AIAA Applied Aerodynamics Conference Jun 28- Jul 1. 1999 Norfolk, Virginia pp 768-778
- Lee C., and Thompson D., 1964 "Fortran Program for Plug Nozzle Design", NASA TM X-53019
- Manski, D., and Hagemann, G., 1996 "Influence of Rocket Design Parameters on Engine Nozzle Efficiencies," *Journal of Propulsion and Power*, Vol. 12, No. 1, pp. 41-47.
- T. Meyer, 1908 "Über zweidimensionale Bewegungsvorgänge in einem Gas, das mit Überschallgeschwindigkeit strömt, Ph.D. thesis, Göttingen.
- Pires, M., 1996 "Escoamento Supersonico em um Expansor Convergente com Corpo Central"- Master Thesis - Instituto Militar de Engenharia-IME.
- Sauer, R. 1947 "General Characteristics of the Flow through Nozzles at Near Critical Speeds" NACA TM 1147.
- Wisse, M.E.N., 2005 "An Asymptotic Analysis of Compressible Base Flow and the Implementation into Linear Plug Nozzles" Ph.D. Thesis, Technische Universiteit Delft, Netherlands.
- Zucrow M.J., Holmann J.D., 1977 "Gas Dynamics", Vols 1 and 2 John Wiley and Sons
- Zucrow M.J., Holmann J.D., 1958 "Aircraft and Missile Propulsion, Vol.1. Wiley, New York.

## 10. RESPONSIBILITY NOTICE

The author is the only responsible for the printed material included in this paper.